JOURNAL OF MATERIALS SCIENCE 26 (1991) 870–880

The morphology, character and strength of the interface in glass fibre–polypropylene composites

C. Y. YUE*, W. L. CHEUNG
Department of Mechanical Engineering, University of Hong Kong, Pokfulam Road, Hong Kong

The interface in clean glass fibre–polypropylene and silane-treated glass fibre–polypropylene pull-out specimens has been studied. The nature of the silane layer on the treated fibres was examined and the influence of agglomerates in the silane layer on the nucleating ability of the fibre surface has been considered. Transcrystalline sheaths of polypropylene were observed in the water-quenched samples but not the air-cooled and 50 °C oven-cooled samples. The nature of the interface and the plane of failure have been determined utilizing optical microscopy and scanning electron microscopy of both the fibre and matrix-failure surfaces. The shrinkage stresses in the air-cooled and oven-cooled clean fibre specimens were relieved by the formation of kink bands. The results suggest the existence of an interphase. The different interfacial strengths in the silane-treated and clean fibre specimens can be explained in terms of the above findings.

1. Introduction

The interfacial properties of a fibre-reinforced composite significantly affect the overall performance of the material. A strong interface allows effective stress transfer between the matrix and the fibres leading to a composite with high strength but low toughness. Conversely, a weak interface would increase the incidence of crack splitting and delamination at the interface during fracture thereby producing a composite with lower strength but high toughness.

In fibre-reinforced semicrystalline thermoplastics, the interfacial properties may also be affected by transcrystalline growth on the fibres. Keller [1] has shown that, apart from the columnar growth form due to restriction by the fibre and the neighbouring spherulites, the structure of the transcrystalline region was identical to a normal spherulite. The transcrystalline region may, however, affect the interfacial properties via the influence that the density of the nucleation sites may have on the bonding between the fibre and the matrix, and via the influence that the effective modulus of the transcrystalline sheath may have on both the stress transfer between the fibre and matrix and on the stress concentration pattern around the fibre. In addition, the mode and path of failure at the interface and hence the mechanical properties of the composite may also be affected by the morphology of the semicrystalline polymer at the fibre surfaces. For these reasons, there has been considerable interest [2–6] in the nucleating ability of semicrystalline polymers on different fibres and substrates. Although *in situ* polymerization of the thermoplastic matrix has been used [6], most existing studies [2–5] are based on work using polymer films and fibres–substrates on a hot stage. The above investigations have primarily been concerned with the classification of substrates with respect to their nucleating ability and the development of an understanding of the role of surface energetics, surface topology, and the need for similarity in crystal structure between the matrix and the substrate on the nucleating capability.

The purpose of the present work is to investigate the character of the silane-treated glass fibre surface, the affect of the silane treatment on the morphology of the polymer at the glass fibre–polypropylene interface, the nature of the interfacial failure in both the absence and the presence of the silane layer, and the affect of the transcrystalline growth on the interfacial bond strength.

2. Experimental details

2.1. Materials

The isotactic homopolymer polypropylene used was Shell Chemical's KM6100 while the silane coupling agent used was Dow Corning's Z-6032. The glass fibres for the experiments were produced by hand drawing a 4 mm diameter E-glass rod after heating the rod in a bunsen burner. The diameter of the resulting glass fibres was about 200 μm.

2.2. Silane layer

Silane treatment of the fibres was carried out in accordance with the manufacturer's instructions. Initially 1% by weight of water was added to the silane coupling agent. This solution was then allowed to age for 24 h before it was further diluted to produce the

* Author to whom correspondence should be addressed at: School of Mechanical and Production Engineering, Nanyang Technological Institute, Nanyang Avenue, Singapore 2263.

0022–2461/90 $03.00 + .12

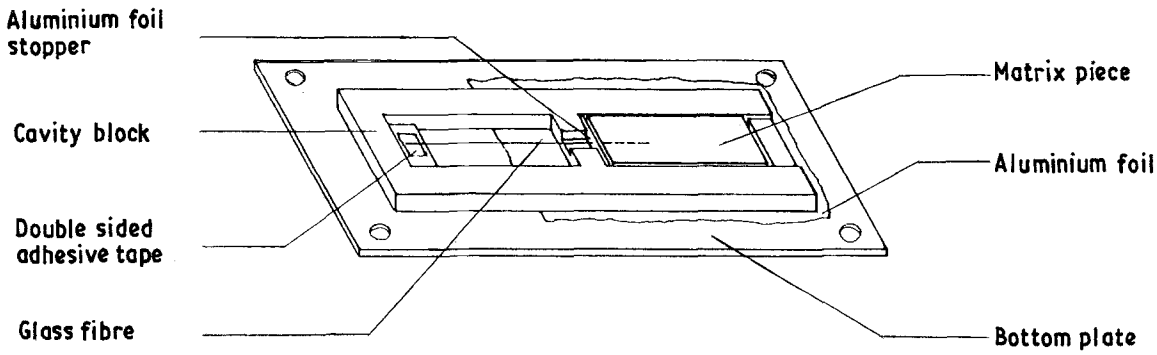

Figure 1 Specimen jig used for compression moulding the pull-out specimens.

treatment, a solution which contained 1% silane (wt%) in water.

To coat the glass fibre with silane, each individual fibre was dipped into the treatment solution for 5 sec. The fibre was then drawn out of the treatment solution in contact with the edge of the solution container so that excess treatment solution could be removed. Such light contact did not scratch or destroy the silane layer on the fibre. To determine the character of the silane layer, some of the treated fibres were sputter coated with gold–palladium and examined in a scanning electron microscope. The thickness and uniformity of the silane coat was determined from scanning electron microscopy of metallographically polished sections of the treated fibres which had been compression moulded between two polypropylene plates.

2.3. Specimen preparation

Pull-out specimens with different embedded lengths were prepared by compression moulding. Initially, rectangular plates (14.5 mm × 49 mm) were cut from compression moulded 2.5 mm thick sheets of polypropylene. A glass fibre of the desired embedded length was then inserted through a pin hole in a small piece (5 mm high) of aluminium foil and placed between two polypropylene plates inside the mould cavity (15 mm × 50 mm × 5 mm) of a specially designed jig (see Fig. 1). The glass fibre was kept in position by the aluminium foil and double sided tape which was used to stick the free end of the fibre onto the jig (see Fig. 1). A recess at the end of the mould cavity in the jig allows excess polymer to flow out during compression moulding so that the specimens were not subjected to very high pressure throughout the moulding process. The jig had five adjacent mould cavities so that five specimens could be produced in each moulding process.

The above set-up was then placed between two mould plates and allowed to heat to 250 °C for 8 min in the compression moulding machine before the mould plates were compressed to effect the moulding. Aluminium foils were placed between the set-up and the mould plates to allow easy removal of the specimen jig and to avoid contamination and heterogeneous nucleation at the mould plate surfaces.

Three cooling schedules were used to vary the morphology of the polypropylene at the fibre–matrix interface. In the water-quenched specimens, tap water was sprayed on both the mould plates immediately upon their removal from the moulding press. For the air-cooled specimens, the moulding set-up was left to cool at room temperature (20 °C). The 50 °C oven-cooled specimens were allowed to cool inside a Heraeus UT5042E oven (which had been preheated to 50 °C) which was switched off once the moulding set-up was placed inside it. Six specimen types were prepared, namely

(a) silane-treated fibre in a water-quenched matrix (TF-WQ)

(b) silane-treated fibre in an air-cooled matrix (TF-AC)

(c) silane-treated fibre in the 50 °C oven-cooled matrix (TF-50 °C)

(d) clean (untreated) fibre in a water-quenched matrix (CF-WQ)

(e) clean fibre in an air-cooled matrix (CF-AC)

(f) clean fibre in the 50 °C oven-cooled matrix (CF-50 °C)

2.4. Testing and examination

After removing the specimens from the mould, a small rectangular piece of cardboard was glued to the free fibre end of the pull-out specimen using epoxy resin to facilitate testing. A free fibre length of 5 mm was maintained between the cardboard and the matrix in all the pull-out specimens. It is important to maintain a constant free length so that the stored energy in the free length at the onset of failure of the interface and at pull-out of the fibre will be the same in all the specimens.

All specimens were left at room temperature for 3 days (to allow the epoxy on the glued cardboard to cure) before they were tested at a cross-head speed of 5 mm min^{-1} in an Instron testing machine. After pull-out, the matrices were sectioned and then microtomed in a direction parallel to the original fibre axis to the hole left by the embedded fibre. These 8 μm thick microtomed sections of the matrix were examined using polarizing optical microscopy to investigate the morphology of the polypropylene at the interface. The nature of the failed interface in the sectioned matrices was examined under an optical microscope. Some of the pulled out fibres and the sectioned matrices were then sputter coated with gold–palladium for examination in the scanning electron microscope (SEM).

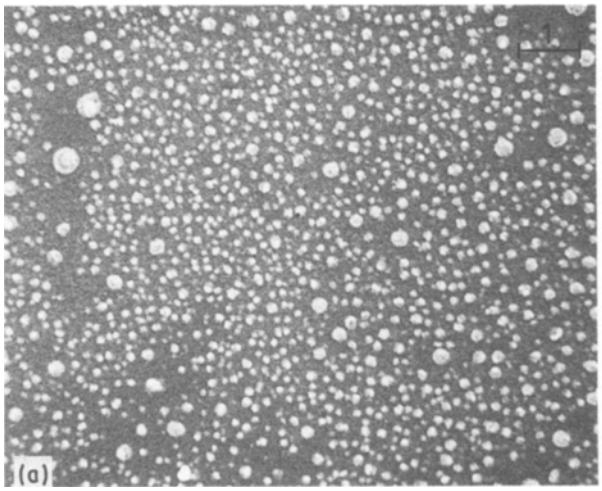

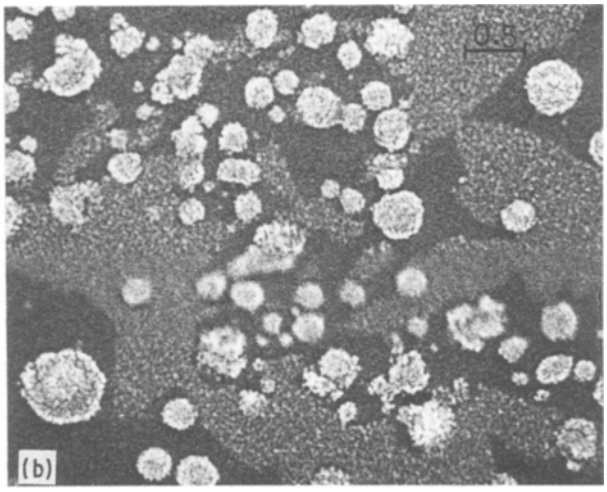

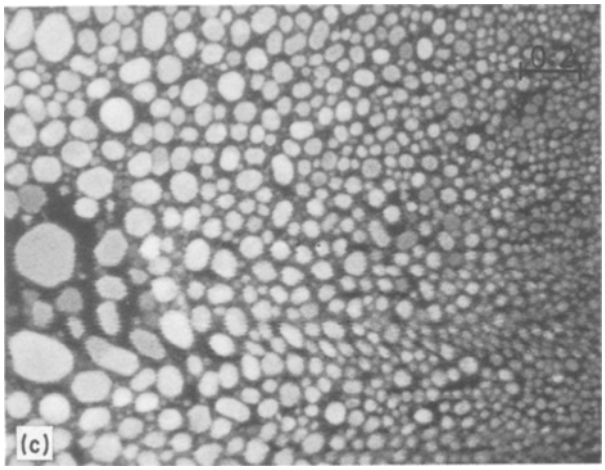

Figure 2 (a) Typical size and distribution of agglomerates on the treated fibre surface, (b) Non-uniform agglomerates on the treated fibre surface, (c) Higher magnification of silane particles within the white patches in (b). (Scale bar in μm.)

Other pulled out fibres and sectioned matrices were etched using a modified permanganic etch [7]. The etch consists of a 60:40 mixture of H_3PO_4 and H_2SO_4 with about 0.5 wt % of potassium permanganate. To investigate the affect of the etch on the silane layer, some treated fibres which had not been embedded in the matrix were also etched and examined in the SEM.

3. Results and discussion

3.1. Character of silane coat

The appearance of the silane coat on the fibre is as shown in Fig. 2. It can be seen that agglomerates of silane exist on the fibre. The presence of the agglomerates arise because of dispersion through emulsification of the silane in the water and is cited in the manufacturer's literature. The size and distribution of the agglomerates over most of the fibre surface was uniform (see Fig. 2a) with agglomerate diameters of less than 0.3 μm. The size and distribution of the agglomerates in some regions of the fibre where some excess treatment solution was present was not, however, uniform (see Fig. 2b) but had large agglomerates (0.3 to 0.5 μm) as well as white patches of very fine agglomerates. A typical higher magnification of such a white patch of very fine agglomerates is as shown in Fig. 2c. It would be interesting to see if these agglomerates affect spherulitic nucleation at the fibre surface in the composite.

Typical micrographs of the polished sections of the treated fibre (which had been embedded in polypropylene) are shown in Fig. 3. The micrograph of the interface in Fig. 3a was taken directly above the polished specimen while that in Fig. 3b was taken with the specimen inclined at 45°. From Fig. 3a it can be seen that the silane coat was about 1 μm thick and was uniform. The agglomerates (in Fig. 2) could not be identified in Fig. 3a which suggests that the agglomerates were not very much higher than the thickness of the surrounding silane coat. It is obvious from Fig. 3b that the surface of the polished specimen was not planar across the fibre–polypropylene interface. This is probably due to the large pressure applied during polishing and to the difference in elastic properties of the fibre, the silane coat and the matrix. The ductile nature of the polished polypropylene surface is apparent. The edge of the silane coat in Fig. 3b was rugged (not flat and featureless as in a brittle failure surface) which suggests that the silane coat was ductile.

The appearance of the silane-coated fibre which had been etched for 5 sec is as shown in Fig. 4. The etch on the fibre was not uniform. It can be seen from the top half of Fig. 4 that the etch initially attacked and dislodged the agglomerates leaving holes in the silane coat. The affect of a longer etching time is typified by the lower half of Fig. 4 which reveals that the silane coat around the holes is removed to expose the bare glass surface. The agglomerates are preferentially removed during the initial stage of etching probably because they comprise clusters of larger and, therefore, more loosely packed silane particles (see Fig. 2) which allowed easier penetration of the etchant to the glass fibre–silane coat interface.

3.2. Interfacial morphology

Typical optical micrographs of the morphology of the polymer at the glass fibre interface is as shown in Fig. 5. The dark bands in Fig. 5 correspond to the original position of the glass fibres in the pull-out

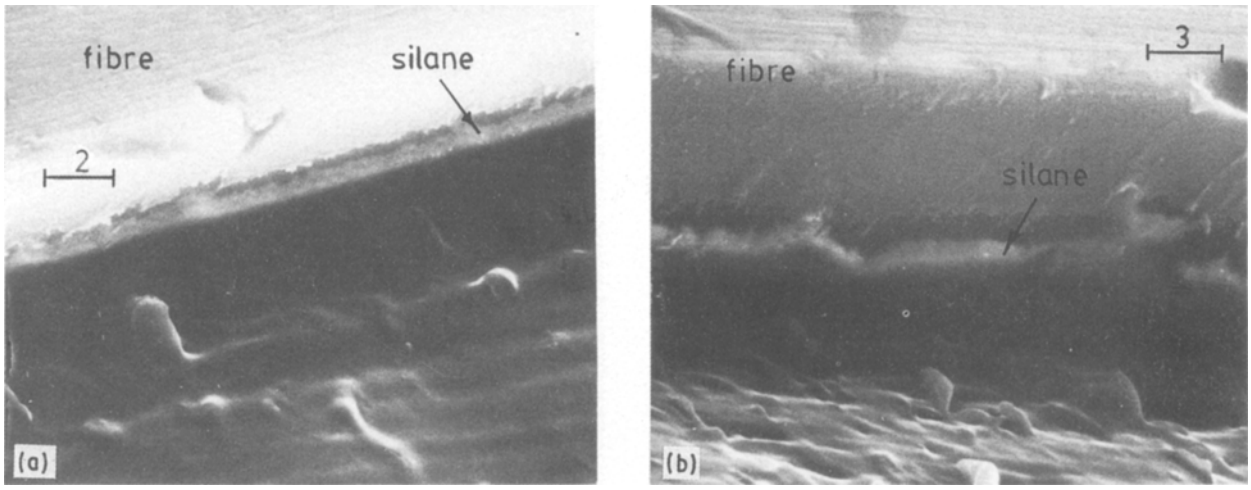

Figure 3 Micrograph of polished treated fibre-polypropylene interface, (a) viewed directly from above, (b) viewed at 45° to the surface of the specimen. (Scale bar in μm.)

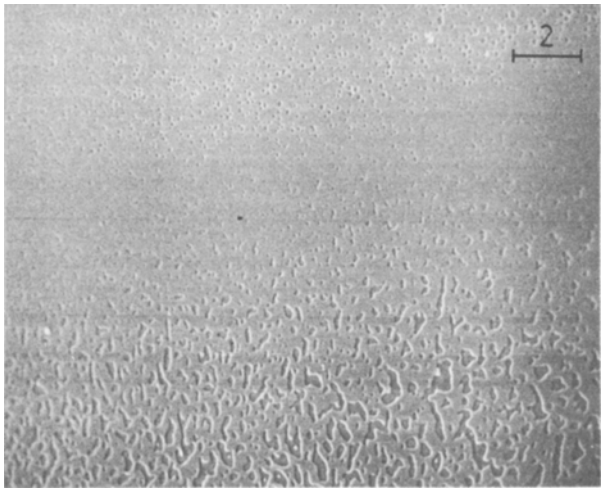

Figure 4 Appearance of etched silane treated glass fibre surface. (Scale bar in μm.)

specimens. Transcrystalline growth similar to that in Fig. 5a was observed along the entire fibre–matrix interface in the water-quenched specimens TF-WQ and CF-WQ. In contrast, no transcrystalline sheath was observed in the air-cooled (TF-AC, CF-AC) and oven-cooled (TF-50 °C, CF-50 °C) specimens. Apart from having spherulites of different sizes, the interfacial morphology in the air-cooled specimens was the same as that in the oven-cooled specimens. The average spherulite diameters in the water quench, air-cooled and oven-cooled specimens are 0.06, 0.26 and 0.40 mm, respectively. For each specimen condition, there was no significant difference in size (within the limits of experimental error) between the transcrystalline regions or spherulites at the interface and the spherulites in the matrix. This suggests that the spherulites at the interface and in the matrix nucleated at the same time.

It was observed that the interfacial morphology was only dependent on the specimen cooling schedule, and that the agglomerates of silane particles on the treated fibre surface had no influence on the interfacial morphology. This suggests that the microrough topography of the treated glass fibre surface due to the agglomerates did not affect the fibre's nucleating ability.

It can be seen from Fig. 5b and the top left hand region in Fig. 5c that some spherulites nucleated at the fibre surfaces of the air-cooled and oven-cooled specimens. Occasionally, isolated pockets of the transcrystalline regions similar to that in the top right-hand region in Fig. 5d could be identified at the interface. It is important to note that some spherulites (similar to that in the top left-hand region in Fig. 5d) nucleated near but not at the fibre–matrix interface. The above observation indicate that glass has poor nucleating ability and this is in agreement with the finding of previous workers [6, 8].

3.3. The nature and character of the interface

The nature and character of the interface was determined by examining both the optical micrographs and SEM fractographs of the failure surfaces in the sectioned matrices of the specimens. Typical optical micrographs of the matrix failure surfaces are as shown in Fig. 6. The bright central bands in Fig. 6 correspond to the interfacial hole left in the matrix by the extracted fibre. Fig. 7 is a micrograph of a typical region within the interface of the CF-AC and CF-50 °C specimen while Fig. 8 consists of some typical micrographs of the etched interfaces in the sectioned matrices.

The nature of the interface in the water-quenched specimens, TF-WQ and CF-WQ, were similar to that in Fig. 6a. The nuclei centres and the base of the spherulites of the transcrystalline regions in the water-quenched specimens are apparent in Fig. 6a. There was no difference in size of the base spherulites of the transcrystalline regions in the treated fibre (TF-WQ) and untreated fibre (CF-WQ) specimens. This further confirms that the agglomerates, due to the silane

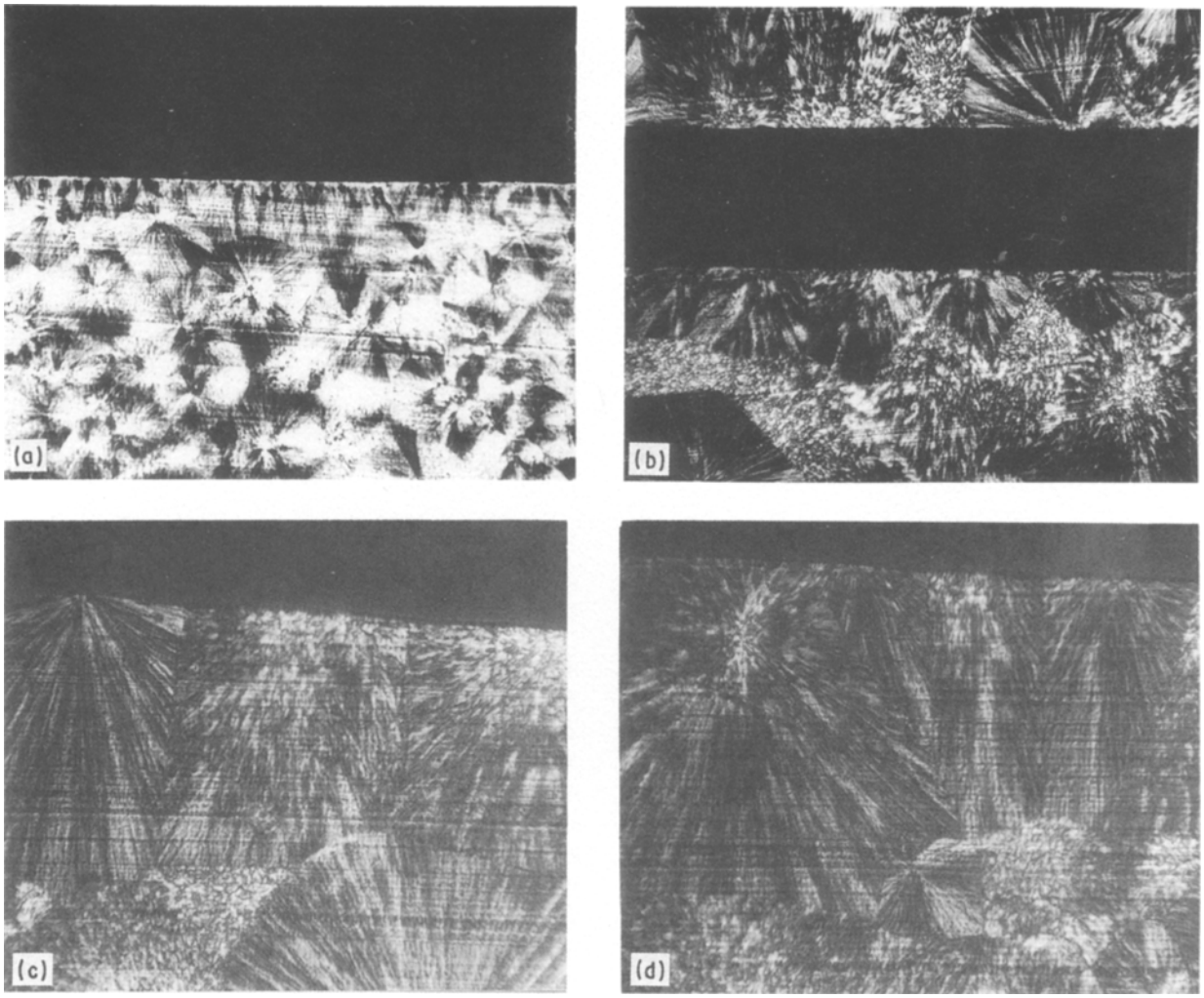

Figure 5 Typical morphology of the polypropylene at the glass fibre interface in specimens, (a) TF-WQ (160 ×), (b) CF-50 °C (80 ×), (c) CF-AC (160 ×), (d) CF-AC (160 ×).

treatment had no affect on the nucleating ability of the fibre.

Occasionally, scratch marks similar to the dark horizontal streaks in the lower left-hand region of the central band in Fig. 6a was evident in the specimens. In contrast to the TF-WQ specimens, the appearance of the entire interfaces in all the CF-WQ specimens were similar to that in Fig. 6a. Most ($\approx$ 80%) of the interface in each TF-WQ specimen was similar to that in Fig. 6b which suggests good bonding between the polymer matrix and the treated fibre. The dark regions within the band in Fig. 6b are dimples due to localized tearing of the polymer from the matrix during pull-out. The nature of these dimples will be discussed in a later section.

The interface in specimens TF-AC and TF-50 °C were similar to that shown in Fig. 6c. Although nuclei of spherulites were sometimes visible, only dimples and scratches similar to that in Fig. 6c were found in all the above specimens. No spherulite boundaries were visible. In contrast, many regions along the interface in specimens CF-AC and CF-50 °C had clearly defined spherulite boundaries which had banded circumferential structure near their perimeters (see Fig. 6d). In addition, unoriented regions, similar to that in the upper left-hand region in Fig. 6d and the vertical middle region in Fig. 7, were frequently trapped between the spherulite boundaries. The micrograph of the circumferential bands (Fig. 7) revealed that the bands were tangential depressions at the perimeter of spherulites at the interface. These tangential depressions were always perpendicular to the radial lamella (see Figs 6d and 7).

The above observations clearly indicated that the circumferential bands only exist in the clean fibre (CF-AC and CF-50 °C) and not the treated fibre specimens. The micrograph of a band which had been etched is as shown in Fig. 8b. It can be seen in Fig. 8b that the radial lamella is continuous across the band. This implies that the circumferential bands are "kink bands" in the radial lamella of the spherulites. Such kink bands only exist at the perimeter of spherulites close to unoriented regions trapped between the boundaries of spherulites (see Figs 6d, 7, 8a, 8b, 8c). No kink bands were observed in the treated fibre specimens although some unoriented regions (similar to that in the bottom right-hand corner of Fig. 8d) also exist at the interface in these specimens.

The kink bands are probably formed during moulding of the specimen. It is known that compressive stresses are set up in the radial direction (with respect to the fibre) when the matrix shrink onto the glass

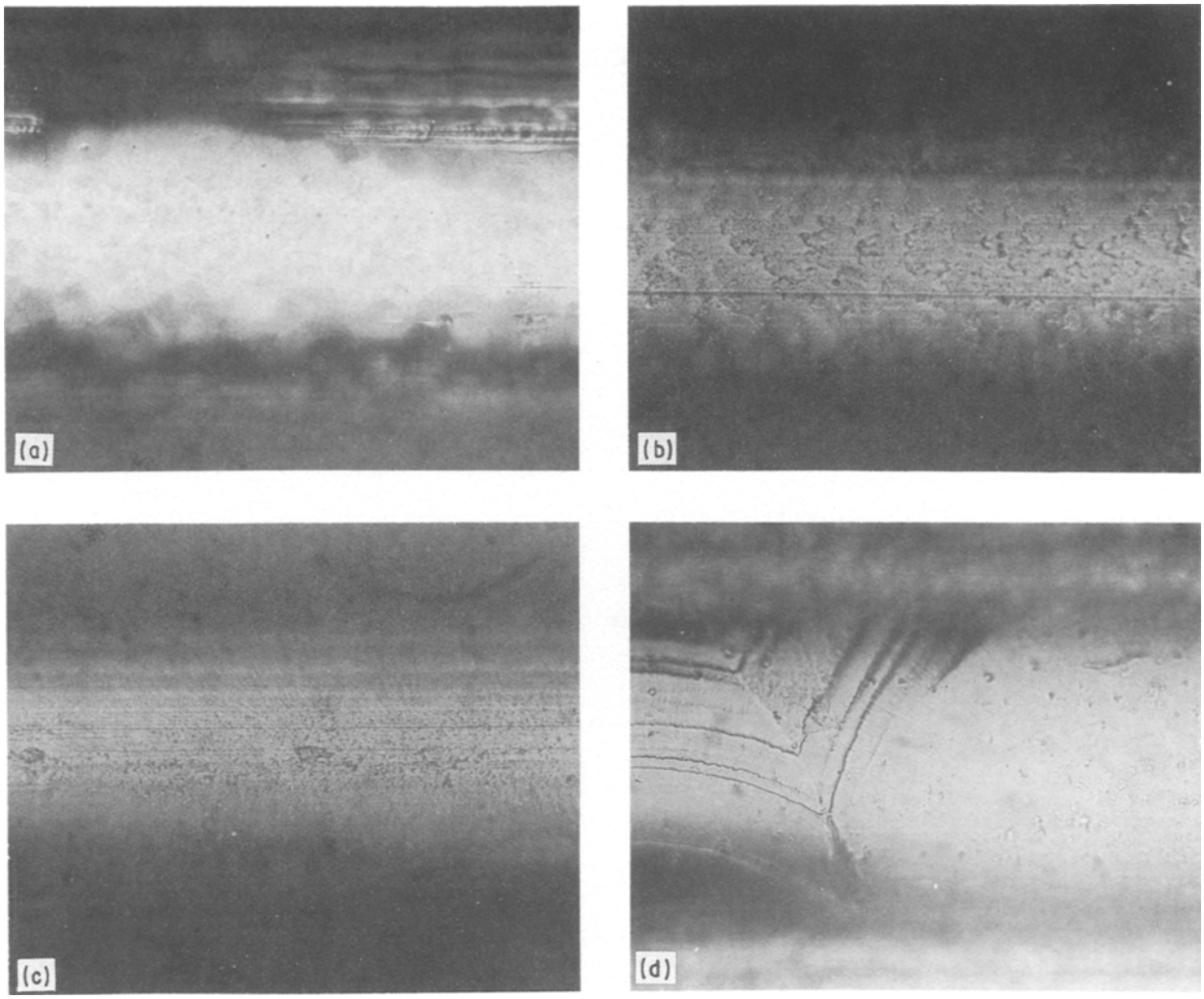

Figure 6 Optical micrographs of the interfacial hole in the sectioned matrices in specimens, (a) TF-WQ, (b) TF-WQ, (c) TF-AC and (d) CF-50 °C, (160 ×).

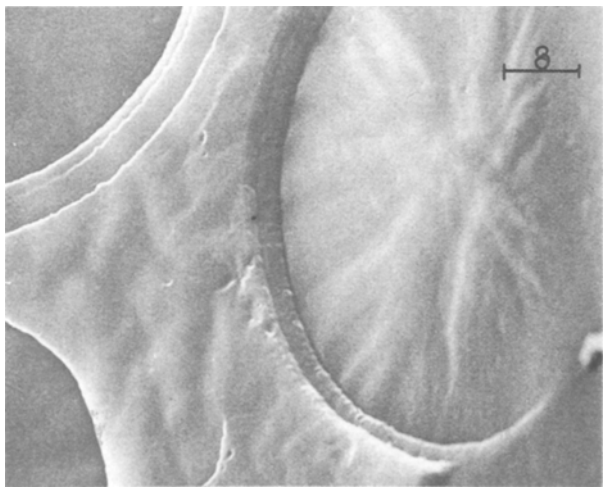

Figure 7 Scanning electron micrograph of a typical circumferential band in specimens CF-AC and CF-50 °C. (Scale bar in μm.)

fibre on solidification from the melt. In addition, residual stresses are set up along the interface in a direction parallel to the fibre axis due to the thermal mismatch between the polypropylene and the glass at the interface. The above thermal mismatch and local variations in the structure of the matrix also causes some localized radial shrinkage [9]. The former compressive stresses cannot be relieved since the glass is rigid. However, under certain conditions the latter two residual stresses can be relieved by shrinkage through the formation of kink bands in the spherulites at the interface.

It is proposed that for kink bands to form, the adhesion between the fibre and the matrix must be poor to allow contraction of the matrix at the interface and there must be no local hindrance to kinking in the spherulite. Hence, the kink bands do not form in specimens TF-AC and TF-50 °C probably because of the better adhesion between the treated fibre and the polypropylene in these specimens (see Figs 6c and 8d). Within the radiating fan-like structure of a sperulite, the lamella packing is expected to be most dense near the nuclei and least dense (i.e. contain more amorphous material between the lamella) near the interspherulitic boundary. Since kinking on shrinkage of the matrix would be easier in regions which are less dense, kink banding is expected to occur preferentially near the interspherulitic boundaries and this is in agreement with the observations in Figs 6d, 7, 8b and 8c. Moreover, kink banding is expected to occur only in spherulites with boundaries adjacent to an unoriented

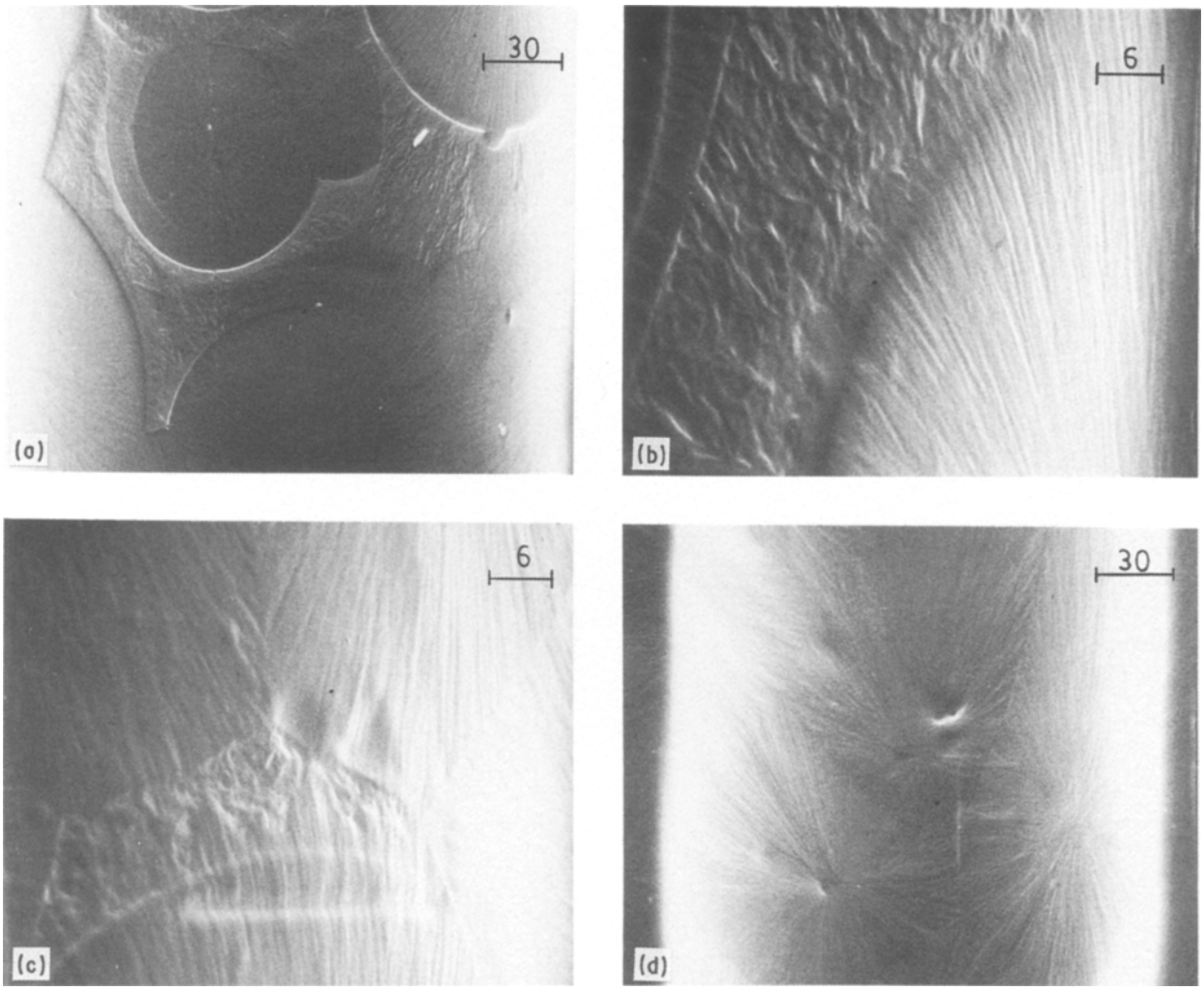

Figure 8 Scanning electron micrographs of etched interfacial holes in specimens, (a), (b) and (c) CF-AC and (d): TF-AC. (Scale bar in μm.)

region. Spherulites with well matched inter-spherulitic boundaries would probably have polymer chains interconnecting adjacent spherulitic lamellae across the common boundaries and are, therefore, unlikely to contract on cooling. This is also in agreement with the observations in Figs 8a, 8c and 8d.

3.4. Fractography and strength of the interface

The plot of debonding force against fibre embedded length is as shown in Fig. 9. The debonding force was taken to be the maximum load in the pull-out test. The interfacial strength of the different specimens as calculated [10] from the experimental results is given in Table I. A full analysis of the results in Fig. 9 will be outlined in a following paper. From Table I, it can be seen that the silane coupling agent on the glass fibres increased the interfacial strength by three times. Despite this, the observed interfacial strengths are very low (cf. a bond strength of 54 MPa in a nylon – E glass fibre system [6]). The very low interfacial strength of the untreated clean fibre specimens was not surprising in view of the inherent poor adhesion of polypropylene to glass. The above results also suggests that the adhesion between polypropylene and the silane layer was poor.

From Table I, it can also be seen that the interfacial strengths in the water-quenched (WQ) specimens are higher than that of the corresponding air-cooled and 50 °C oven-cooled specimens. It is not known if the higher interfacial strength in the water-quenched specimens could be attributed to the presence of the transcrystalline sheath and the higher density of nuclei centres in these specimens. This is because the matrix

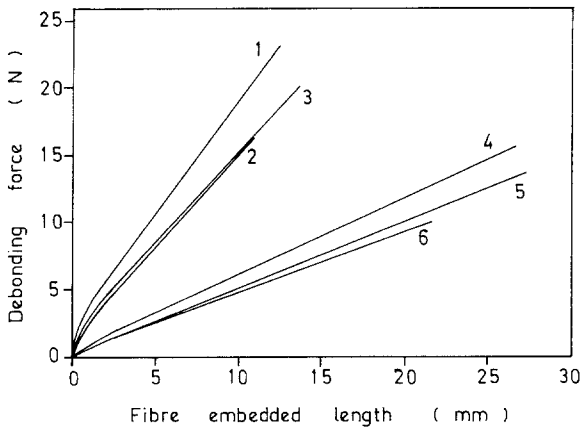

Figure 9 Plot of debonding force against fibre embedded length for all the specimens: (1) TF-WQ, (2) TF-AC, (3) TF-50 °C, (4) CF-WQ, (5) CF-AC, (6) CF-50 °C.

TABLE I Interfacial strength of the specimens

Specimen	TF-WQ	TF-AC	TF-50 °C	CF-WQ	CF-AC	CF-50 °C
Interfacial strength (MPa)	3.5	2.7	2.7	1.0	0.9	0.8

shrinkage pressure on the fibres, which can affect the interfacial strength, is different [9] in the water-quenched, the air-cooled and 50 °C oven-cooled specimens.

Fractography of both the extracted fibres and the interfacial holes in the sectioned matrices of the specimen was carried out to determine the plane of failure and to obtain more information on the nature of the interface. The micrograph of a sectioned matrix in specimen CF-AC is as shown in Fig. 10a. The appearance of the interfacial hole in specimens CF-50 °C and CF-AC was the same. Apart from the kink bands at the outer perimeter of the spherulites, there were some rough white patches of deformed matrix particles near the spherulite centres (see Fig. 10a). In contrast, the interfacial holes in specimens CF-WQ were featureless apart from some random white spots of deformed matrix particles.

The micrographs in Figs 10b, 10c and 10d depict some typical appearance of the extracted fibre surface in all the clean untreated fibre specimens. It is apparent in Fig. 10b that in addition to some small lumps of matrix, there were many dark as well as white patches on the fibre surface. Higher magnification of the fibre surface (see Fig. 10c and 10d) revealed that the dark regions correspond to the bare surface of the glass fibre. There are many white spots within the bare surface (see Fig. 10c) which probably correspond to the actual points of contact between the matrix and the fibre that had been deformed during the debonding and pull-out process. More than 50% of the extracted fibre surface had white patches of "matrix" material similar to that in Fig. 10d. This is very surprising as it suggests a large contact area between the matrix and the fibre. The above observations further suggest that the interfacial strength should be high since failure is within the matrix, which is contradictory to the results in Table I. The lack of any evidence of ductile deformation on the "matrix" material in Fig. 10d suggests that this "matrix" material probably has a different structure from the polymer in

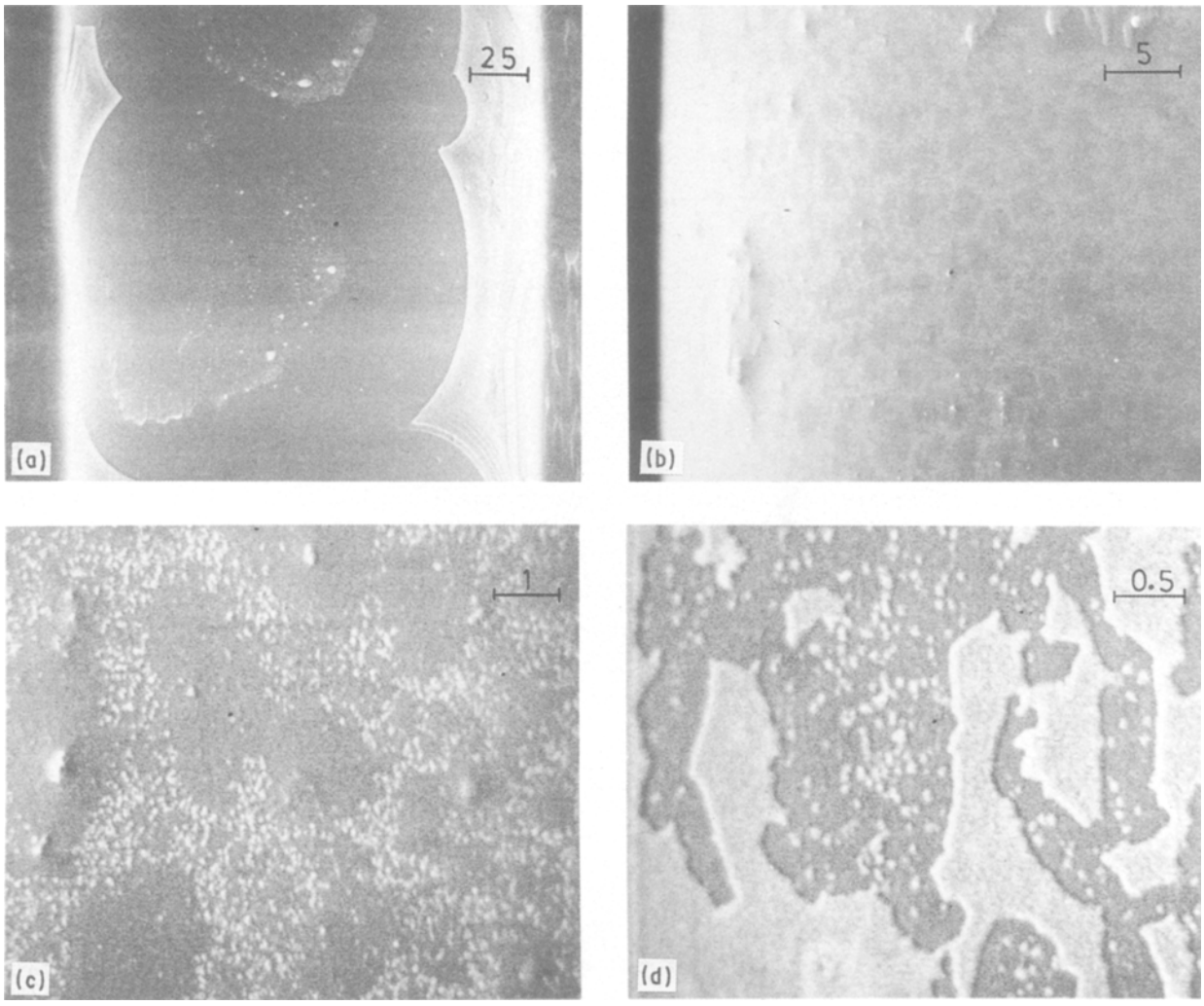

Figure 10 Scanning electron micrographs of some clean fibre specimens, (a) sectioned matrix CF-AC, (b) pulled out fibre CF-50 °C, (c) fibre surface CF-AC, (d) fibre surface CF-50 °C. (Scale bar in μm.)

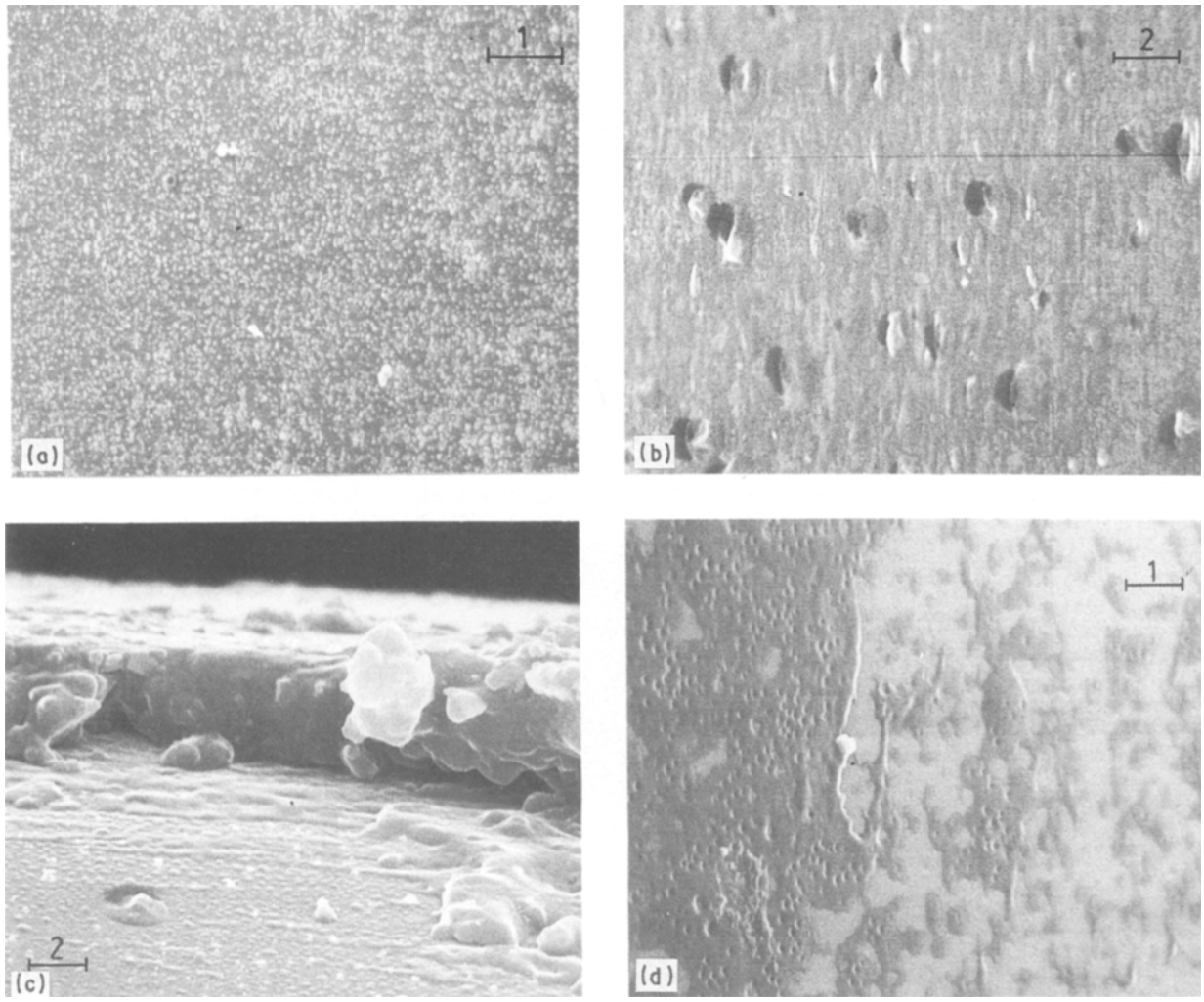

Figure 11 Scanning electron micrographs of some extracted treated fibres, (a) TF-WQ, (b) TF-50 °C, (c) TF-WQ, (d) etched fibre surface TF-WQ. (Scale bar in μm.)

the bulk matrix. The above observations probably suggest that an interphase region exist at the surface of the fibres and that failure occurs at the interface between the interphase and the polymer matrix. It is possible that this interphase is a "weak boundary layer" [11].

There was no difference in the appearance of the surface of the extracted fibre in all the treated fibre specimens. Typical high magnification micrographs of the extracted treated fibre surface are as shown in Fig. 11a, 11b and 11c. In some regions of the fibre, failure was between the silane layer and the matrix so that the small agglomerates of the silane layer was apparently beneath a thin uniform sheath of matrix (see right-hand portion of Fig. 11c). The appearance of such a surface in a TF-WQ specimen after etching for 5 min is as shown in Fig. 11d. The etchant removes both the matrix and the silane layer. Remnants of the silane layer in which the agglomerates had been removed are apparent on the etched surface (see Fig. 11d and cf. Fig. 4). This confirmed that a silane layer exists below fracture surfaces similar to that in the right-hand portion of Fig. 11c. No dominant failure mechanism appear to exist on the extracted fibre surface.

Two typical high magnification micrographs of the surfaces of the interfacial holes in the sectioned matrix are as shown in Fig. 12. The failure surface in Fig. 12a contain many shallow dimples and probably correspond to a region which was originally in contact with a fibre surface region in Fig. 11a. The shallow dimples are probably created from failure at the silane layer–matrix interface in these regions. The failure surface in Fig. 12b contains some deformed polymer which appear as white regions. Some of these white regions probably contain some detached silane agglomerates. Such a matrix failure surface probably matches the fibre failure surfaces similar to that in Fig. 11b and on the right-hand portion of Fig. 11c.

Occasionally tears in the silane layer were observed on the fibre failure surface (see dark regions in Fig. 13a). In one particular specimen with large silane agglomerates, a torn film was evident on the fibre failure surface (see upper region in Fig. 13b). A close examination of the left hand corner of the torn region in Fig. 13b (see Fig. 13c) suggests that a two-layer structure exist on the fibre. The two layers are probably the interphase (or thin "matrix" layer) on the surface and the silane layer which contain agglomerates below the surface layer.

From Figs 11 and 13, it is apparent that the adhesion between the silane layer and the glass fibre is better than the adhesion between the silane layer and

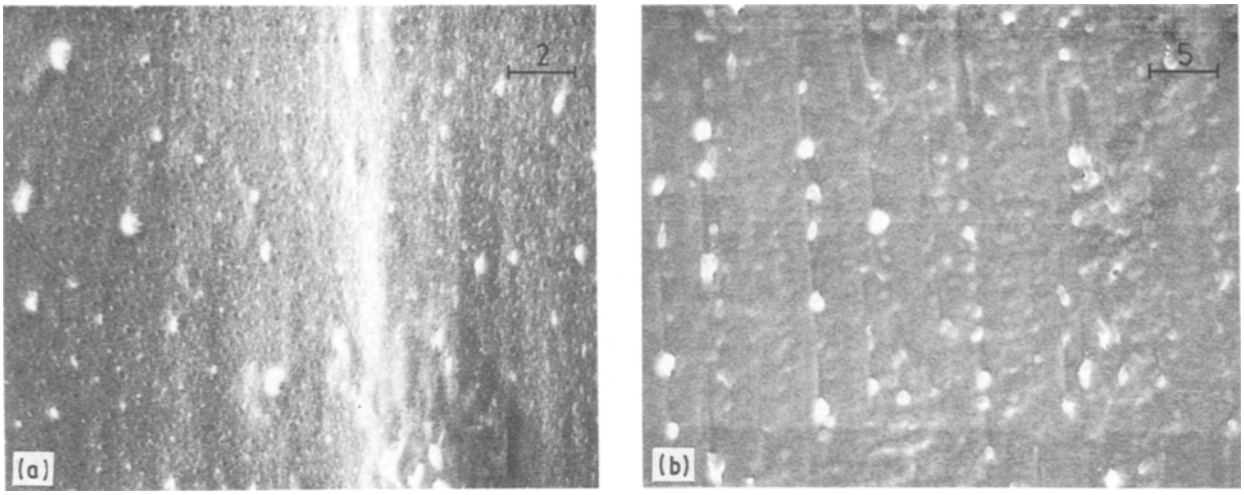

Figure 12 Scanning electron micrographs of typical matrix failure surface, (a) TF-50 °C, (b) TF-AC. (Scale bar in μm.)

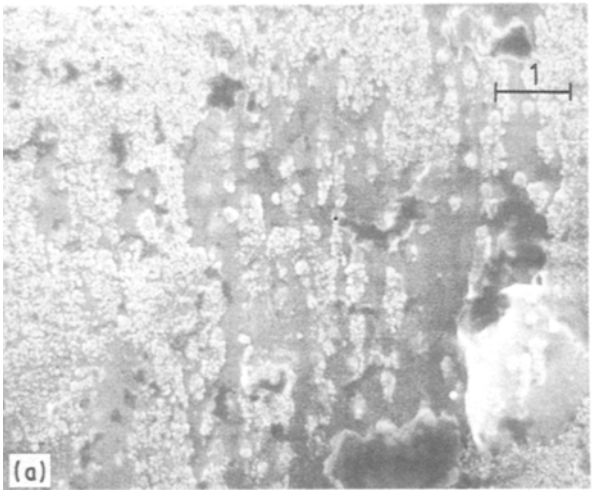

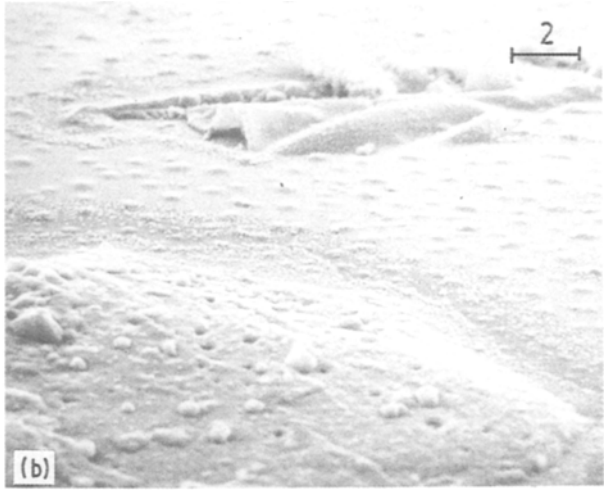

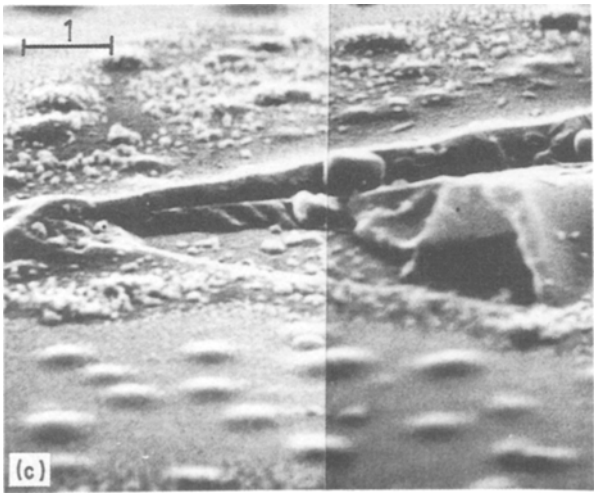

Figure 13 (a) Tears in the silane layer in specimen TF-50 °C, (b) Tears in the silane layer and in the interphase in specimen TF-AC, (c) Higher magnification of the left-hand corner of the torn region in (b). (Scale bar in μm.)

the polypropylene matrix. This is because no failure was observed at the interface between the silane layer and the glass surface. Since failure in the treated fibre specimen sometimes occurred in the matrix (see Fig. 11c), the adhesion between the silane layer and the polymer is better than the adhesion between the untreated glass fibre and the polymer in the clean fibre specimens (see Fig. 10). Therefore, the interfacial strength in the treated fibre specimens would be higher than the interfacial strength in the untreated clean fibre specimens. This is in agreement with the results in Table I.

4. Conclusions

In addition to a thin uniform silane layer, agglomerates consisting of many loose silane particles form on the fibre surface when the fibre is dip coated in the silane solution. These agglomerates had no influence on the nucleating ability of the fibre surface since the interfacial morphology of both the treated and clean fibre specimens were the same for a given preparation schedule. Transcrystalline sheaths formed around the fibres in the water-quenched specimens. There were many spherulites around the interface which did not nucleate at the fibre surface in the air-cooled and 50 °C oven-cooled specimens. The shrinkage stresses at the matrix–fibre interface in the clean fibre specimens were relieved through the formation of kink bands at the perimeter of the spherulites. The real contact area between the matrix and the fibre in the clean fibre specimens was small. There was evidence for the existence of an interphase in the above specimens. In the

treated fibre specimens, failure either occurred at the interface between the silane layer and the matrix, or within the matrix, or probably at the interface between an interphase and the matrix. The interfacial strength of the treated fibre specimens was higher than the interfacial strength of the clean fibre specimens.

Acknowledgements

The assistance of Mr S. M. Kwok, Mr H. W. Chua and Mr P. I. Wong in conducting some of the experiments is gratefully acknowledged. One of us, WLC, was supported on a University studentship during the course of this work.

References

1. A. KELLER, *J. Polym. Sci.* **15** (1955) 31.
2. R. H. BURTON and M. J. FOLKES, in "Mechanical Properties of Reinforced Thermoplastics" edited by D. W. Clegg and A. A. Collyer (Elsevier, London, 1986) p. 269.
3. D. CAMPBELL and M. M. QAYYUM, *J. Polym. Sci., Polym. Phys. Edn* **18** (1980) 83.
4. S. Y. HOBBS, *Nature Phys. Sci.* **234** (1971) 12.
5. A. M. CHATTERJEE, F. P. PRICE and S. NEWMAN, *J. Polym. Sci. Polym. Phys. Edn* **13** (1975) 2369.
6. T. BESSELL and J. B. SHORTALL, *J. Mater. Sci.* **10** (1975) 2035.
7. D. R. NORTON and A. KELLER, *Polymer* **26** (1985) 704.
8. R. H. BURTON and M. J. FOLKES, *Plast. Rubber Process. Appl.* **3** (1983) 129.
9. W. L. CHEUNG and C. Y. YUE, paper in preparation.
10. C. Y. YUE and W. L. CHEUNG, Seventh International Conference on Deformation, yield and fracture of polymers, Churchill College, Cambridge (1988).
11. L. H. SHARPE, *J. Adhesion* **4** (1972) 51.

Received 31 July 1989
and accepted 19 February 1990